


# Textural features of $^{18}\text{F}$ -fluorodeoxyglucose positron emission tomography scanning in diagnosing aortic prosthetic graft infection

Ben R. Saleem<sup>1</sup>  · Roelof J. Beukinga<sup>2,3</sup> · Ronald Boellaard<sup>2</sup> · Andor W. J. M. Glaudemans<sup>2</sup> · Michel M. P. J. Reijnen<sup>4</sup> · Clark J. Zeebregts<sup>1</sup> · Riemer H. J. A. Slart<sup>2,3</sup>

Received: 12 September 2016 / Accepted: 9 December 2016 / Published online: 24 December 2016  
© The Author(s) 2016. This article is published with open access at Springerlink.com

## Abstract

**Background** The clinical problem in suspected aortoiliac graft infection (AGI) is to obtain proof of infection. Although  $^{18}\text{F}$ -fluorodeoxyglucose ( $^{18}\text{F}$ -FDG) positron emission tomography scanning (PET) has been suggested to play a pivotal role, an evidence-based interpretation is lacking. The objective of this retrospective study was to examine the feasibility and utility of  $^{18}\text{F}$ -FDG uptake heterogeneity characterized by textural features to diagnose AGI.

**Methods** Thirty patients with a history of aortic graft reconstruction who underwent  $^{18}\text{F}$ -FDG PET/CT scanning were included. Sixteen patients were suspected to have an AGI (group I). AGI was considered proven only in the case of a positive bacterial culture. Positive cultures were found in 10 of the 16 patients (group Ia), and in the other six patients, cultures remained negative (group Ib). A control group was formed of 14 patients undergoing  $^{18}\text{F}$ -FDG PET for other reasons (group II). PET images were assessed using conventional maximal

standardized uptake value (SUVmax), tissue-to-background ratio (TBR), and visual grading scale (VGS). Additionally, 64 different  $^{18}\text{F}$ -FDG PET based textural features were applied to characterize  $^{18}\text{F}$ -FDG uptake heterogeneity. To select candidate predictors, univariable logistic regression analysis was performed ( $\alpha = 0.16$ ). The accuracy was satisfactory in case of an  $\text{AUC} > 0.8$ .

**Results** The feature selection process yielded the textural features named variance ( $\text{AUC} = 0.88$ ), high grey level zone emphasis ( $\text{AUC} = 0.87$ ), small zone low grey level emphasis ( $\text{AUC} = 0.80$ ), and small zone high grey level emphasis ( $\text{AUC} = 0.81$ ) most optimal for distinguishing between groups I and II. SUVmax, TBR, and VGS were also able to distinguish between these groups with AUCs of 0.87, 0.78, and 0.90, respectively. The textural feature named short run high grey level emphasis was able to distinguish group Ia from Ib ( $\text{AUC} = 0.83$ ), while for the same task the TBR and VGS were not found to be predictive. SUVmax was found predictive in distinguishing these groups, but showed an unsatisfactory accuracy ( $\text{AUC} = 0.75$ ).

**Conclusion** Textural analysis to characterize  $^{18}\text{F}$ -FDG uptake heterogeneity is feasible and shows promising results in diagnosing AGI, but requires additional external validation and refinement before it can be implemented in the clinical decision-making process.

Ben R. Saleem and Roelof J. Beukinga contributed equally to this work.

**Electronic supplementary material** The online version of this article (doi:10.1007/s00259-016-3599-7) contains supplementary material, which is available to authorized users.

✉ Ben R. Saleem  
r.b.saleem@gmail.com

<sup>1</sup> Department of Surgery, Division of Vascular Surgery, University of Groningen, University Medical Center Groningen, P.O. Box 30 001, 9700 RB Groningen, The Netherlands

<sup>2</sup> Nuclear Medicine and Molecular Imaging, University of Groningen, University Medical Center Groningen, Groningen, The Netherlands

<sup>3</sup> Department of Biomedical Photonic Imaging (BMPI), University of Twente, Enschede, The Netherlands

<sup>4</sup> Department of Surgery, Rijnstate Hospital, Arnhem, The Netherlands

**Keywords**  $^{18}\text{F}$ -FDG PET · Aortic prosthetic graft infection · Textural features

## Background

Aortoiliac prosthetic graft infection (AGI) is a severe complication after prosthetic graft placement, which is associated

with high morbidity and mortality [1–5]. Positive bacterial cultures, either from percutaneous aspirated perigraft fluid or from surgically obtained material, are considered the gold standard for diagnosing AGI [1–5]. However, a perigraft abscess or fluid collection is not always present, and even if present it may not always be suitable for puncture. The diagnosis of AGI, therefore, remains an important challenge.

Non-invasive  $^{18}\text{F}$ -fluorodeoxyglucose positron emission tomography ( $^{18}\text{F}$ -FDG PET) imaging may play an important role in increasing the diagnostic accuracy of infectious diseases with inherent elevated intracellular glucose metabolism [6–11]. The PET images can either be evaluated semi-quantitatively using the maximal standardized uptake value (SUV<sub>max</sub>) and the tissue-to-background ratio (TBR), and visually using the visual grading scale (VGS). For diagnostic assessments which are based on a combination of these parameters, our group reported a high sensitivity (up to 91%), but a low specificity (up to 64%) [10], which was also confirmed by others [6, 7, 11]. Additionally, there is no consensus with respect to the interpretation of these  $^{18}\text{F}$ -FDG PET findings. Recently, SUV<sub>max</sub> >8 in the perigraft area was suggested as the cutoff value for proof of an infection of a thoracic prosthetic graft [12]. However, this value must be interpreted with caution as this study was conducted in only nine patients and scans were not acquired according to European Association of Nuclear Medicine (EANM) recommendations [13]. Moreover, our group found the above-mentioned quantitative measures when used as so-called cutoff values to determine infection to be of modest utility in the diagnosis of AGI [14]. As a consequence, more accurate quantification methods are needed. Since a heterogeneous uptake is associated with infection, the distribution pattern of  $^{18}\text{F}$ -FDG activity may help identify AGI with a higher diagnostic precision [6]. A powerful tool for quantifying such distribution is textural analysis, which may provide valuable information regarding biological heterogeneity. The concept of textural analysis is generally based on the spatial arrangement of voxels in a predefined volume of interest (VOI). Spatial heterogeneity can be depicted from different spatial interrelationships on  $^{18}\text{F}$ -FDG PET scans. Within the field of clinical oncology, textural analysis already has yielded promising results in predicting response by quantifying intra-tumoral heterogeneity [15–23].

In the current study, we introduced the principle of textural analysis into the field of infectious diseases and aimed to investigate feasibility and accuracy of textural features to diagnose AGI.

## Methods

### Design of the study

For this retrospective analysis we included all patients ( $n = 30$ ) from a prospective database of patients with a history of

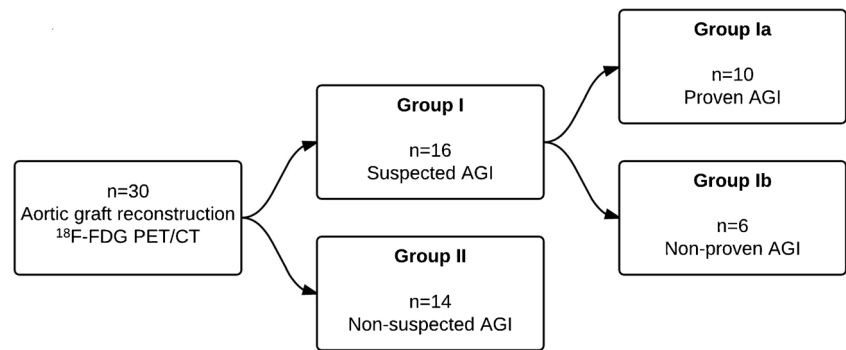
aortoiliac prosthetic graft reconstruction who underwent  $^{18}\text{F}$ -FDG PET/CT at our tertiary referral center between December 2009 and May 2015. Medical charts were analysed to identify those patients with a clinical suspicion of an AGI. An AGI was clinically suspected in case of undefined fever, a deep wound infection, persisting high laboratory infection parameters [e.g. erythrocyte sedimentation rate, white blood cell count, and/or C-reactive protein (CRP)], or a combination of these factors. AGI was considered proven only in cases where a positive bacterial culture of material was obtained from peri-prosthetic samples obtained during diagnostic work-up or surgery. Sixteen patients were clinically suspected to have an AGI (group I) of which 10 had a positive culture (group Ia) and six had a negative culture (group Ib). The remaining 14 patients underwent a  $^{18}\text{F}$ -FDG PET/CT scan because of cancer staging and were used as control group. Figure 1 shows a flow chart of the patient disposition.

Patient characteristics and information about the initial operation, type of graft material, clinical symptoms and laboratory parameters at the time of  $^{18}\text{F}$ -FDG PET imaging, and definite type of treatment were collected from the medical records. Co-morbidities were defined as recommended by the Ad Hoc Committee on Reporting Standards [24]. This study was approved by the institutional ethical review board (METc 2015/082). Patients' data were analysed anonymously.

### $^{18}\text{F}$ -FDG PET imaging and analysis

Non-gated PET/CT imaging was performed with a dedicated integrated PET/CT system (Biograph mCT PET/CT, Siemens, Knoxville, TN, USA). All patients fasted overnight with no restrictions on drinking water and with a minimum fasting time of 6 h prior to PET/CT.  $^{18}\text{F}$ -FDG was administered intravenously with a weight-based activity of 3 MBq/kg. Sixty minutes after tracer injection, patients were positioned on the camera table with the arms in upright position. PET images were acquired with 3 min per bed position. An initial low dose CT scan was performed to ensure that the region of interest was included in the field of view, where after an inspiration breath-hold low-dose CT for attenuation correction was performed with 100 kVp and 30 mAs. Image data were reconstructed using standard methods and images were standardized according to EANM guidelines [13].

An experienced nuclear medicine physician assessed the  $^{18}\text{F}$ -FDG PET images, including VGS, SUV<sub>max</sub> and TBR. The five-point VGS was graded as follows: grade 0,  $^{18}\text{F}$ -FDG uptake similar to that in the background; grade I, low  $^{18}\text{F}$ -FDG uptake, comparable with inactive muscles and fat; grade II, moderate  $^{18}\text{F}$ -FDG uptake, clearly visible and higher than uptake by inactive muscles and fat; grade III, strong  $^{18}\text{F}$ -FDG uptake, but distinctly less than the physiologic urine bladder activity; and grade IV, very strong  $^{18}\text{F}$ -FDG uptake, comparable with the physiologic urinary activity of the

**Fig. 1** Flow chart of patient disposition

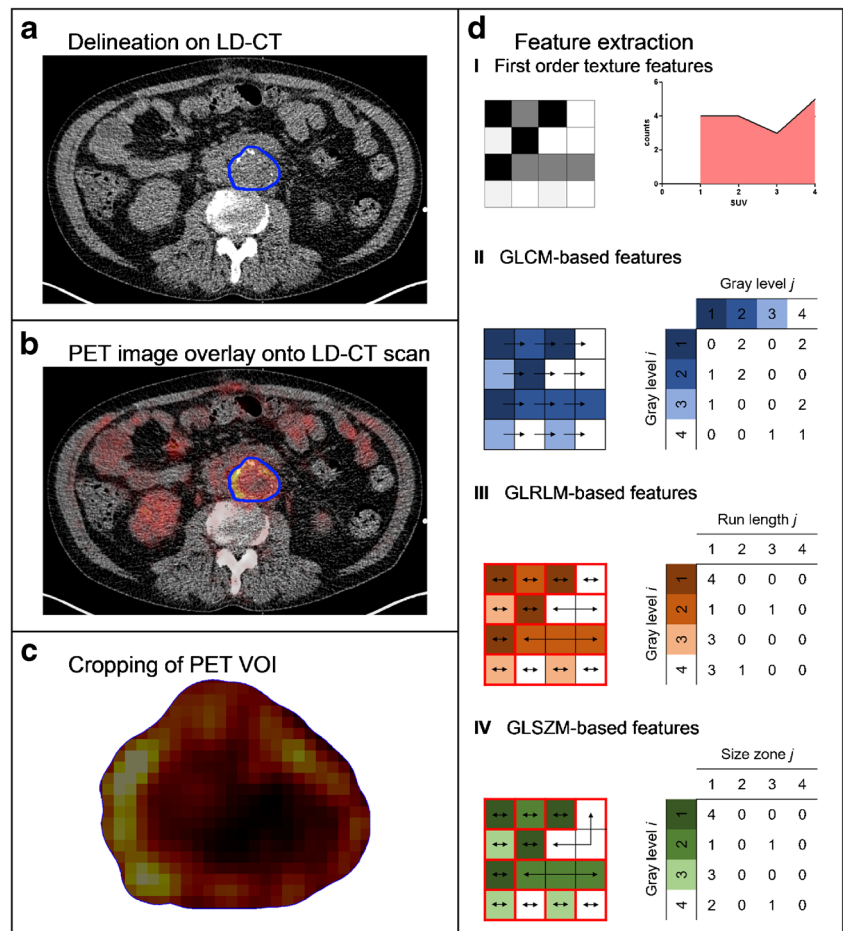
bladder [10, 25]. A VOI was drawn around the area of the vascular prosthesis to calculate the SUVmax. SUVmax corresponded to the voxel with the highest  $^{18}\text{F}$ -FDG uptake. The TBR was defined as the SUVmax divided by the mean SUV of the caval vein (blood pool).

### Volume of interest

$^{18}\text{F}$ -FDG PET based textural features to characterize heterogeneity of  $^{18}\text{F}$ -FDG uptake in the aortic prosthetic graft were measured for each patient. Figure 2 displays the image processing and extraction of all textural features ( $n = 64$ ) from a

predefined VOI. VOIs were manually delineated (Fig. 2a) by two independent experienced nuclear medicine physicians on axial planes of the low-dose CT to enclose three-dimensional coverage of the entire suspected prosthetic graft, using PMOD 3.6 software (PMOD Inc., Zurich, Switzerland). However, as the partial volume effect may cause the activity to be smeared out over a larger area than the actual structure, and the total number of counts is preserved, we also included high uptake regions around the graft material with clear contamination of activity from the graft (spill over). Moreover, we assessed whether  $^{18}\text{F}$ -FDG uptake was physiological or non-physiological based on the CT-based anatomical location

**Fig. 2** **a** Manual delineation on LD-CT; **b** Overlay of colour-mapped PET image onto LD-CT; **c** Cropping of PET VOI; **d** Feature extraction; I) Global assessment of tonal distribution by means of first order textural features; II) Assessment of pairwise arrangement of voxels by means of construction of grey level co-occurrence matrix (GLCM); III) Assessment of alignment of voxels with the same intensity by means of construction of grey level run-length matrix (GLRLM); IV) Assessment of characteristics of homogenous zones by means of construction of grey level size-zone matrix (GLSZM)



and excluded high uptake regions with clear spill-in effects from physiological neighbouring tissues such as the kidneys, ureter, and urine bladder. Although this VOI definition leads to analysis on the whole prosthetic graft volume, we chose for this definition since analysis of the most-diseased segment of the aortic graft would require a semi-objective identification of the  $^{18}\text{F}$ -FDG-avid area [13]. Additionally, prosthetic grafts of group II do often not contain a  $^{18}\text{F}$ -FDG-avid area, which, therefore, complicates the comparison with Group I. After VOI delineation, the PET/CT imaging data and VOI delineations were loaded into Matlab 2014b (Mathworks, Natick, MA, USA) for processing and analysis (Fig. 2b). The VOI delineations were then registered to the PET images. PET voxels, which were enclosed for  $\geq 50\%$  coverage, were considered to be part of the suspected prosthetic graft (Fig. 2c). For noise reduction, SUV was discretized with fixed 0.5 g/mL increments according to Doane's optimal bin width [26]. Textural analysis was performed on the cropped PET VOI. To find the influence of the volume of the VOI on textural features the Pearson correlation coefficient was calculated.

### Textural features extraction

Figure 2d and supplemental table 1 provide a full overview of all 64 analysed textural features. We extracted 19 first order textural features (based on the grey level distribution, but without spatial information of voxels). Texture can be characterized by replications of (small) texture elements. These texture elements consist of contiguous voxels with certain spatial and intensity properties. We obtained the distributions of three different texture elements, i.e. the grey level co-occurrence (or

spatial dependence) matrix (GLCM) for pairwise arrangement of voxels [27], the grey level run-length matrix (GLRLM) for alignment of voxels with an identical intensity [28], and the grey level size-zone matrix (GLSZM) for characteristics of homogeneous zones [29]. From these matrices, we extracted 46 s order textural features (which are thus based on spatial information of the grey levels). These textural features were extracted with a voxel-to-voxel distance offset of  $d=1$  and directional analysis was performed with a connectivity of 26 voxels (analysis in 13 angular directions). All extracted textural features were normalized to the range [0,1]. To determine the influence of noise, it was tested whether noise was equally distributed among the groups and the correlation between noise and each textural feature was computed. Therefore, a sphere of 3 cm in diameter was drawn in the liver; the coefficient of variation was determined as noise parameter.

### Statistical analysis

Baseline characteristics are presented as mean  $\pm$  standard deviation or percentages. To select candidate predictors to identify infection, univariable logistic regression analysis was performed. All potential predictors that met the Akaike Information Criterion (AIC) were considered significant [30]. To discourage overfitting, the AIC is based on rewarding goodness of fit and penalizing complexity in the model. The AIC requires  $\chi^2 > 2 df$ , i.e. when considering a predictor with one degree of freedom  $df$ ; this implies a significance level  $\alpha = P(\chi^2 \geq 2) = 0.16$  [31]. The accuracy of all candidate predictors was measured by the area under the receiver operating characteristic curve (AUC). Textural features were considered to have a good accuracy in case of an AUC  $> 0.8$ . Moreover, textural feature values may be subject to inter-observer variability in delineation of the prosthesis. Textural features were considered stable in case of a minimum acceptable excellent agreement indicated by an intra-class correlation coefficient (ICC) level of 0.75 [32]. To obviate multicollinearity among all significant, accurate, and stable considered textural features, the pairwise Pearson correlation coefficient was evaluated. When the correlation of a pair of variables was  $> 0.8$ , the variable with the lowest AUC was excluded from the set of features chosen for AGI characterization. Data were collected and analysed using IBM SPSS 20.0 software (IBM Corp, Armonk, NY, USA).

## Results

### Baseline patient characteristics

Twenty-four (80%) of the 30 patients were male. The mean age at the time of PET/CT scanning was 68 years, ranging from 42 to 77 years. Patient characteristics are

**Table 1** Patient characteristics

Total	Group Ia	Group Ib	Group II
N	10	6	14
Sex			
Male	7	4	13
Female	3	2	1
Age; years, mean (range)	66 (42–76)	68 (58–77)	70 (52–77)
Co-morbidity*			
Diabetes mellitus	6	2	5
Tobacco use	7	5	12
Hypertension	8	4	3
Hyperlipemia	6	4	7
Cardiac disease	4	5	12
Renal disease	7	2	11
Pulmonary disease	9	3	8

\* Defined according to the Ad Hoc Committee on Reporting Standards [24]



described in Table 1. There were no significant differences between the groups with respect to demographic data (Pearson Chi-Square test). Table 2 shows the organisms obtained from culture in group I. Twenty-one (70%) patients were initially treated because of aneurysmal disease and the remaining for occlusive disease. Operative details of the primary operation are listed in Table 3. The time intervals between the initial operation and the  $^{18}\text{F}$ -FDG PET scan for diagnosing AGI were  $43.6 \pm 42.0$  months and  $75.5 \pm 55.7$  months for group Ia and Ib, respectively. In group Ia and Ib, antibiotic treatment was initialized before the  $^{18}\text{F}$ -FDG PET scan was performed in eight (80%) and five (83%) patients with  $2.2 \pm 31.5$  days and  $25.8 \pm 30.0$  days since clinical suspicion of AGI, respectively. Pre-scan serum glucose levels ranged from 4.0 to 7.7 mmol/L (median 5.6 mmol/L, mean 5.7 mmol/L), including the diabetic patients. Two patients in group Ib died within 30 days after surgical removal of the suspected graft due to postoperative complications. No autopsy was performed on these two patients. The other four patients had no signs of infection during further follow-up (mean 7 months), suggesting that these grafts were correctly classified as non-infected. Nine patients in group II died during follow up ( $67.6 \pm 37.5$  months) mainly because of malignancy, without any sign of infection.

### Visual grading scale

VGS for group I was  $3.25 \pm 1.06$ . VGS was  $3.50 \pm 0.71$  for group Ia and  $2.83 \pm 1.47$  for group Ib. The VGS for group II was  $1.4 \pm 0.94$ . The VGS was found to differ significantly between groups I and II ( $P < 0.01$ ), with an AUC of 0.90.

**Table 2** Bacteriology of infected prosthetic graft material in group I

	Culture obtained from:		
	Perigraft fluid N (10)	Surgery N (6)	Total N (%)
Group Ia	5	5	10 (63)
Group Ib	5	1	6 (37)
Organism			
Candida albicans	2	1	3
Coagulase-negative staphylococci	–	1	1
Enterococcus faecalis/faecium	1	2	3
Escherichia coli	–	1	1
Granulicatella adiacens	1	–	1
Nocardia farcinica	–	1	1
Proteus mirabilis	–	1	1
Proteus vulgaris	–	1	1
Staphylococcus aureus	2	–	2

**Table 3** Graft location and material at initial operation

	Group Ia N (%)	Group Ib N (%)	Group II N (%)
Underlying disease			
Aneurysmatic	5 (50)	4 (57)	12 (86)
Occluding	5 (50)	2 (43)	2 (14)
Graft location			
Aortoiliac	6 (60)	5 (83)	13 (93)
Iliofemoral	4 (40)	1 (17)	1 (7)
Type of reconstruction			
Open	9 (90)	6 (100)	8 (57)
Endovascular	1 (10)	0 (0)	6 (43)
Graft material			
Dacron®	7 (70)	6 (100)	7 (50)
PTFE	2 (20)	0 (0)	0 (0)
EVAR	1 (10)	0 (0)	7 (50)
- Medtronic®	1 (10)	0 (0)	4 (29)
- Cook-Zenith®	0 (0)	0 (0)	3 (21)

PTFE polytetrafluoroethylene; and EVAR endovascular aortic repair

However, the VGS appeared not to differ significantly between groups Ia and Ib ( $P = 0.26$ ), with an AUC of 0.64.

### Maximum standardized uptake value

The SUVmax for group I was  $7.01 \pm 2.31$  compared to  $4.17 \pm 1.86$  for group II. The SUVmax for group Ia was  $7.72 \pm 2.22$  compared to  $5.83 \pm 2.09$  for group Ib. SUVmax was found to be predictive in distinguishing group I from II ( $P = 0.01$ ) with an accuracy of AUC = 0.87. SUVmax was also able to

distinguish group Ia from Ib ( $P = 0.13$ ), but with an unsatisfactory accuracy of  $AUC = 0.75$ .

**Tissue-to-background ratio**

TBR for group I was  $4.57 \pm 2.14$ . TBR was  $4.86 \pm 2.15$  for group Ia and  $3.82 \pm 2.14$  for group Ib. The TBR for group II was  $2.94 \pm 1.54$ . The TBR was found to differ significantly between groups I and II ( $P = 0.06$ ) with an  $AUC$  of 0.78, but appeared not to differ significantly between groups Ia and Ib ( $P = 0.35$ ) with an  $AUC$  of 0.70.

**Textural features**

Textural analysis was completed for 30 patients. No significant correlations were found between volume and texture features. Fifteen (22%) of the studied textural features, were found to be robust for inter-observer variability in delineation of the prosthesis and were suitable for AGI prediction. Four textural features fulfilled all selection criteria ( $P$ -value  $< 0.16$  in the univariable analysis,  $AUC > 0.80$ , and  $ICC > 0.75$ ) in distinguishing suspected from non-suspected graft infection (Table 4). The high-grey-level-zone-emphasis and small-zone-high-grey-level-emphasis were found to correlate, hence the small-zone-high-grey-level-emphasis was excluded from further analysis since this variable had the lowest  $AUC$  of the two. Variance, high-grey-level-zone-emphasis, and small-zone-low-grey-level-emphasis remained predictive for AGI characterization with  $AUC$ s of 0.88, 0.87, and 0.81, respectively. Short-run-high-grey-level-emphasis was the only

textural feature to fulfil all selection criteria in distinguishing proven (group Ia) from non-proven (group Ib) infection (Table 4). The  $AUC$  of the short-run-high-grey-level-emphasis was 0.83, allowing a sensitivity of 80% and a specificity of 100% using an optimal threshold of 0.70. The short-run-high-grey-level-emphasis value for group Ia was  $20.45 \pm 11.02$  compared to  $10.05 \pm 3.92$  for group Ib,  $16.55 \pm 10.25$  for group I, and  $7.65 \pm 4.38$  for group II. Figure 3 shows a coronal view of  $^{18}\text{F}$ -FDG PET images of proven and non-proven infected prosthetic grafts and the corresponding values of the conventional measures, and the selected textural features. No significant differences were found in the amount of noise between group I and II ( $P = 0.34$ ) neither between group Ia and Ib ( $P = 0.10$ ).

**Discussion**

This study investigates the relationship between  $^{18}\text{F}$ -FDG uptake heterogeneity in the aortic prosthetic graft, as characterized by textural features, and AGI. This study shows that textural analysis of AGI is feasible and may increase the accuracy to diagnose AGI compared to conventional assessment.

In this study, several textural features were found to be robust for inter-observer variability in delineation of the prosthesis and seem to be suitable for AGI prediction. Short-run-high-grey-level-emphasis, which is highly dependent on the occurrence of short runs (and thus a heterogeneous  $^{18}\text{F}$ -FDG uptake) with high grey levels, was the only textural feature to

**Table 4** Regression analysis results, accuracy, and robustness of the selected variables

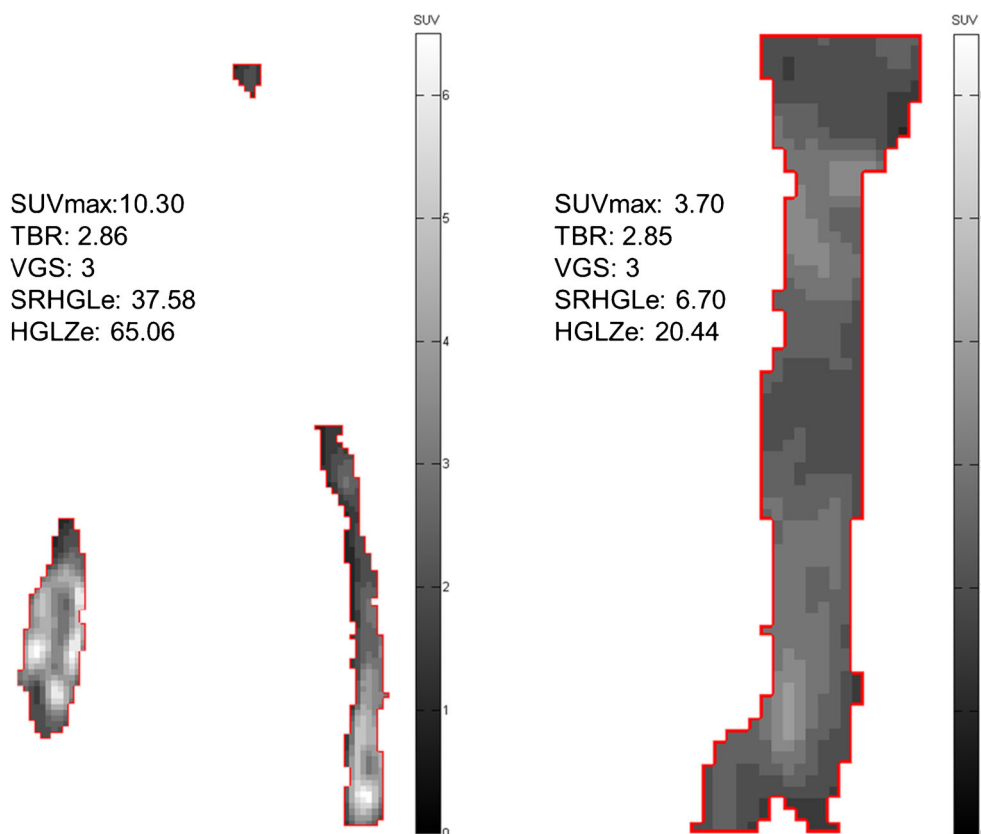
Variable	I vs. II		Ia vs. Ib		ICC
	<i>P</i> -value	AUC	<i>P</i> -value	AUC	
Conventional measures					
Maximal standardized uptake value	<b>0.01</b>	<b>0.87</b>	<b>0.13</b>	0.75	
Tissue to background ratio	<b>0.06</b>	0.78	0.35	0.70	
Visual grading scale	<b>&lt;0.01</b>	<b>0.90</b>	0.26	0.64	
First order textural features					
Variance	<b>0.01</b>	<b>0.88</b>	0.17	0.70	<b>0.85</b>
GLRLM-based textural features					
Short run high grey level emphasis*	<b>0.02</b>	0.79	<b>0.07</b>	<b>0.83</b>	<b>0.75</b>
GLSZM-based textural features					
High grey level zone emphasis†	<b>0.01</b>	<b>0.87</b>	<b>0.12</b>	0.78	<b>0.83</b>
Small zone low grey level emphasis	<b>0.01</b>	<b>0.80</b>	0.16	0.73	<b>0.86</b>
Small zone high grey level emphasis	<b>0.04</b>	<b>0.81</b>	<b>0.15</b>	0.75	<b>0.79</b>

Variables satisfying  $P$ -value  $< 0.16$ ,  $AUC > 0.8$ , and  $ICC > 0.75$  are given in bold  
 GLRLM grey level run-length matrix; and GLSZM grey level size-zone matrix

\* Textural feature selected for separating group Ia from Ib

† Textural feature selected for separating group I from II

**Fig. 3** A coronal view of  $^{18}\text{F}$ -FDG PET images of proven and non-proven infected prosthetic aortic grafts, and the corresponding values of conventional measures and the set of textural features chosen for AGI characterization. Abbreviations: SRHGLe = short-run-high-grey-level-emphasis; HGLZe = high-grey-level-zone-emphasis



distinguish proven (group Ia) from non-proven (group Ib) infection. The short-run-high-grey-level-emphasis demonstrated higher values for the studied infected prosthetic grafts compared to the uninfected prosthetic grafts. This finding, therefore, supports the hypothesis that a high and heterogeneous  $^{18}\text{F}$ -FDG uptake is associated with infected prosthetic grafts. The short-run-high-grey-level-emphasis was most efficient in identifying AGI within the suspected group, whereas for the same task the performances of SUVmax, TBR, and VGS measurements were all limited.

Diagnoses based on the standard parameters could significantly distinguish between patients being suspected (group I) and non-suspected (group II) of having AGI. VGS showed the highest accuracy of all studied parameters, indicating that these groups can sufficiently be distinguished without textural analysis. However, among these standard parameters, only the SUVmax was able to distinguish group Ia from Ib. Spacek et al. visually interpreted  $^{18}\text{F}$ -FDG uptake as “intense”, “inhomogeneous”, or “none” and found intense focal  $^{18}\text{F}$ -FDG uptake to be a significant predictor for AGI [9], which confirms that SUVmax results were found significant in the current study. However, as was also supported by our previous study [14], the accuracy of SUVmax was moderate and insufficient for changing clinical decision-making. Of interest, Keidar et al. visually assessed patterns of uptake for non-infected vascular grafts in patients undergoing a  $^{18}\text{F}$ -FDG

PET for other reasons than suspected AGI [33]. A diffuse homogeneous uptake was observed in 67 grafts (63%) and heterogeneous uptake was observed in 31 grafts (29%). Nine grafts (8%) demonstrated no  $^{18}\text{F}$ -FDG uptake and none of the grafts displayed focal  $^{18}\text{F}$ -FDG uptake. Keidar et al. hypothesized that diffuse  $^{18}\text{F}$ -FDG PET uptake in non-infected grafts is a result of a local sterile inflammatory process around the prosthesis due to a foreign body-related reaction, and also related to the type of implanted material. Moreover, Berger et al. found the mentioned standard parameters largely to overlap in infected and uninfected central vascular grafts [34], which confirms our findings that conventional parameters are not sufficient in distinguishing these groups.

The current study demonstrated the association of high and heterogeneous  $^{18}\text{F}$ -FDG uptake with AGI; however, due to the relatively small patient cohort it seems not applicable for clinical decision making yet. Nevertheless, this finding is of utmost importance, since it warrants studies with larger, prospective patient cohorts with the construction of multivariable prediction models. Such studies should focus on the textural features, which were found robust for inter-observer variability in the current study. One of the most important limitations in testing the utility of textural analysis in the diagnosis of AGI is the fact that 80% of the patients received antibiotic therapy at the time of scanning, which may have yielded false-negative cultures. However, this bias is the result of the

clinical reality, since the omission of antibiotic therapy could adversely affect patients and this issue is related to each study predicting AGI. Moreover, routine microbiologic techniques can sometimes fail to isolate the microorganism from perigraft material [35, 36]. Sonication techniques have been described to identify indolent gram-positive microorganisms by using ultrasound energy to agitate particles from the graft sample for microbiology [35, 36]. However, we did not apply these sonication techniques in this retrospective study because they were not available in our hospital. In addition, the used definition for VOI leads to analysis on the whole prosthetic graft volume, which possibly results in an underestimation of the predictive value of the textural features. However, as we mentioned earlier, we chose for this definition since analysis of the most-diseased segment of the aortic graft would require a semi-objective identification of the  $^{18}\text{F}$ -FDG-avid area [13] and since group II does not contain such an area.

## Conclusion

Textural analysis to characterize  $^{18}\text{F}$ -FDG uptake heterogeneity is feasible and shows promising results in diagnosing AGI and can encourage further research to facilitate implementation of automated textural analysis algorithms into clinical practice. Further research regarding the construction, refinement, and validation of prediction models in larger prospective cohorts is required before it can be implemented in the clinical decision-making process.

$^{18}\text{F}$ -FDG PET,  $^{18}\text{F}$ -fluorodeoxyglucose positron emission tomography; AGI, aortic graft infection; AIC, Akaike information criterion; AUC, area under the receiver operating characteristic curve; CRP, C-reactive protein; CT, computed tomography; EANM, European Association of Nuclear Medicine; EVAR, endovascular aortic repair; GLCM, grey level co-occurrence matrix; GLRLM, grey level run-length matrix; GLSZM, grey level size-zone matrix; ICC, intra-class correlation coefficient; PTFE, polytetrafluoroethylene; SUVmax, maximal standardized uptake value; TBR, tissue-to-background ratio; VGS, visual grading scale; and VOI, volume of interest

**Authors' contributions** Conception and design: BRS, RJB, RB, CJZ, and RHJAS

Provision of study materials or patients: BRS, RJB, CJZ, and RHJAS

Collection and assembly of data: BRS, RJB, CJZ, and RHJAS

Data analysis and interpretation: BRS, RJB, RB, AWJMG, MMPJR, CJZ, and RHJAS

Manuscript writing: BRS, RJB, RB, AWJMG, MMPJR, CJZ, and RHJAS

Final approval of manuscript: BRS, RJB, RB, AWJMG, MMPJR, CJZ, and RHJAS

## Compliance with ethical standards

**Funding** No external funding was received.

**Conflict of interests** None.

**Informed consent** Informed consent was not required (retrospective study).

**Open Access** This article is distributed under the terms of the Creative Commons Attribution 4.0 International License (<http://creativecommons.org/licenses/by/4.0/>), which permits unrestricted use, distribution, and reproduction in any medium, provided you give appropriate credit to the original author(s) and the source, provide a link to the Creative Commons license, and indicate if changes were made.

## References

1. Valentine RJ. Diagnosis and management of aortic graft infection. *Semin Vasc Surg.* 2001;14:292–301.
2. O'Connor S, Andrew P, Batt M, Becquemin JP. A systematic review and meta-analysis of treatments for aortic graft infection. *J Vasc Surg.* 2006;44:38–45.
3. Perera GB, Fujitani RM, Kubaska SM. Aortic graft infection: update on management and treatment options. *Vasc Endovasc Surg.* 2006;40:1–10.
4. Saleem BR, Meerwaldt R, Tielliu IF, Verhoeven EL, van den Dungen JJ, Zeebregts CJ. Conservative treatment of vascular prosthetic graft infection is associated with high mortality. *Am J Surg.* 2010;200:47–52.
5. Legout L, D'Elia PV, Sarraz-Bournet B, et al. Diagnosis and management of prosthetic vascular graft infections. *Med Mal Infect.* 2012;42:102–9.
6. Fukuchi K, Ishida Y, Higashi M, et al. Detection of aortic graft infection by fluorodeoxyglucose positron emission tomography: comparison with computed tomographic findings. *J Vasc Surg.* 2005;42:919–25.
7. Keidar Z, Engel A, Hoffman A, Israel O, Nitecki S. Prosthetic vascular graft infection: the role of  $^{18}\text{F}$ -FDG PET/CT. *J Nucl Med.* 2007;48:1230–6.
8. Lauwers P, Van den Broeck S, Carp L, Hendriks J, Van Schil P, Blockx P. The use of positron emission tomography with  $^{18}\text{F}$ -fluorodeoxyglucose for the diagnosis of vascular graft infection. *Angiology.* 2007;58:717–24.
9. Spacek M, Belohlavek O, Votrubova J, Sebesta P, Stadler P. Diagnostics of “non-acute” vascular prosthesis infection using  $^{18}\text{F}$ -FDG PET/CT: our experience with 96 prostheses. *Eur J Nucl Med Mol Imaging.* 2009;36:850–8.
10. Bruggink JL, Glaudemans AW, Saleem BR, et al. Accuracy of FDG-PET-CT in the diagnostic work-up of vascular prosthetic graft infection. *Eur J Vasc Endovasc Surg.* 2010;40:348–54.
11. Keidar Z, Nitecki S. FDG-PET in prosthetic graft infections. *Semin Nucl Med.* 2013;43:396–402.
12. Tokuda Y, Oshima H, Araki Y, et al. Detection of thoracic aortic prosthetic graft infection with  $^{18}\text{F}$ -fluorodeoxyglucose positron emission tomography/computed tomography. *Eur J Cardiothorac Surg.* 2013;43:1183–7.
13. Boellaard R, O'Doherty MJ, Weber WA, et al. FDG PET and PET/CT: EANM procedure guidelines for tumour PET imaging: version 1.0. *Eur J Nucl Med Mol Imaging.* 2010;37:18–200.
14. Saleem BR, Berger P, Vaartjes I, et al. Modest utility of quantitative measures in  $^{18}\text{F}$ -fluorodeoxyglucose positron emission tomography scanning for the diagnosis of aortic prosthetic graft infection. *J Vasc Surg.* 2015;61:965–71.
15. Eary JF, O'Sullivan F, O'Sullivan J, Conrad EU. Spatial heterogeneity in sarcoma  $^{18}\text{F}$ -FDG uptake as a predictor of patient outcome. *J Nucl Med.* 2008;49:1973–9.



16. Yu H, Caldwell C, Mah K, et al. Automated radiation targeting in head-and-neck cancer using region-based textural analysis of PET and CT images. *Int J Radiat Oncol Biol Phys.* 2009;75:618–25.
17. Yu H, Caldwell C, Mah K, Mozeg D. Coregistered FDG PET/CT-based textural characterization of head and neck cancer for radiation treatment planning. *IEEE Trans Med Imaging.* 2009;28:374–83.
18. El Naqa I, Grigsby P, Apte A, et al. Exploring feature-based approaches in PET images for predicting cancer treatment outcomes. *Pattern Recognit.* 2009;42:1162–71.
19. van Velden FHP, Cheebsumon P, et al. Evaluation of a cumulative SUV-volume histogram method for parameterizing heterogeneous intratumoural FDG uptake in non-small cell lung cancer PET studies. *Eur J Nucl Med Mol Imaging.* 2011;38:1636–47.
20. Tixier F, Le Rest CC, Hatt M, et al. Intratumor heterogeneity characterized by textural features on baseline 18F-FDG PET images predicts response to concomitant radiochemotherapy in esophageal cancer. *J Nucl Med.* 2011;52:369–78.
21. Vaidya M, Creach KM, Frye J, Dehdashti F, Bradley JD, El Naqa I. Combined PET/CT image characteristics for radiotherapy tumor response in lung cancer. *Radiother Oncol.* 2012;102:239–45.
22. Tan S, Kligerman S, Chen W, et al. Spatial-temporal [18F]FDG-PET features for predicting pathologic response of esophageal cancer to neoadjuvant chemoradiation therapy. *Int J Radiat Oncol Biol Phys.* 2013;85:1375–82.
23. Zhang H, Tan S, Chen W, et al. Modelling pathologic response of oesophageal cancer to chemoradiation therapy using spatial-temporal 18F-FDG PET features, clinical parameters, and demographics. *Int J Radiat Oncol Biol Phys.* 2014;88:195–203.
24. Rutherford RB, Baker JD, Ernst C, et al. Recommended standards for reports dealing with lower extremity ischemia: revised version. *J Vasc Surg.* 1997;26:517–38.
25. Saleem BR, Pol RA, Slart RH, Reijnen MM, Zeebregts CJ. 18F-Fluorodeoxyglucose positron emission tomography/CT scanning in diagnosing vascular prosthetic graft infection. *Biomed Res Int.* 2014;471971:1–8.
26. Doane DP. Aesthetic frequency classifications. *Am Stat.* 1976;30:181–3.
27. Haralick RM, Shanmugam K, Dinstein I. Textural features for image classification. *IEEE Trans Syst Man Cybern.* 1973;3:610–21.
28. Galloway MM. Textural analysis using gray level run lengths. *Comput Graphics Image Process.* 1975;4:172–9.
29. Thibault G, Fertil B, Navarro C, Pereira S, Cau P, Levy N, et al. Textural indexes and gray level size zone matrix. Application to Cell Nuclei Classification. *Pattern Recognit Inf Process.* 2009:140–145.
30. Akaike H. A new look at the statistical model identification. *IEEE Trans Autom Control.* 1974;19:716–23.
31. Steyerberg EW. Clinical prediction models. A practical approach to development, validation, and updating. New York: Springer; 2009.
32. Cicchetti DV. Guidelines, criteria, and rules of thumb for evaluating normed and standardized assessment instruments in psychology. *Psychol Assess.* 1994;6:284–90.
33. Keidar Z, Pirmisashvili N, Leiderman M, Nitecki S, Israel O. 18F-FDG uptake in noninfected prosthetic vascular grafts: incidence, patterns, and changes over time. *J Nucl Med.* 2014;55:392–5.
34. Berger P, Vaartjes I, Scholtens A, Moll FL, De Borst GJ, De Keizer B, et al. Differential FDG-PET uptake patterns in uninfected and infected central prosthetic vascular grafts. *Eur J Vasc Endovasc Surg.* 2015;50:376–83.
35. Bergamini TM, Bandyk DF, Govostis D, Vetsch R, Towne JB. Identification of *Staphylococcus epidermidis* vascular graft infection: a comparison of culture techniques. *J Vasc Surg.* 1989;9:665–70.
36. Tollefson DF, Bandyk DF, Kaebnick HW, Seabrook GR, Towne JB. Surface biofilm disruption. Enhanced recovery of microorganisms. *Arch Surg.* 1987;122:38–43.